Function of the HVCN1 proton channel in airway epithelia and a naturally occurring mutation, M91T

David Iovannisci, Beate Illek, and Horst Fischer

Children's Hospital Oakland Research Institute, Oakland, CA 94609

Airways secrete considerable amounts of acid. In this study, we investigated the identity and the pH-dependent function of the apical H^+ channel in the airway epithelium. In pH stat recordings of confluent JME airway epithelia in Ussing chambers, Zn-sensitive acid secretion was activated at a mucosal threshold pH of ~7, above which it increased pH-dependently at a rate of 339 ± 34 nmol × h^{-1} × cm^{-2} per pH unit. Similarly, H^+ currents measured in JME cells in patch clamp recordings were readily blocked by Zn and activated by an alkaline outside pH. Small interfering RNA–mediated knockdown of HVCN1 mRNA expression in JME cells resulted in a loss of H^+ currents in patch clamp recordings. Cloning of the open reading frame of HVCN1 from primary human airway epithelia resulted in a wild-type clone and a clone characterized by two sequential base exchanges (452T>C and 453G>A) resulting in a novel missense mutation, M91T HVCN1. Out of 95 human genomic DNA samples that were tested, we found one HVCN1 allele that was heterozygous for the M91T mutation. The activation of acid secretion in epithelia that natively expressed M91T HVCN1 required ~0.5 pH units more alkaline mucosal pH values compared with wild-type epithelia. Similarly, activation of H^+ currents across recombinantly expressed M91T HVCN1 required significantly larger pH gradients compared with wild-type HVCN1. This study provides both functional and molecular indications that the HVCN1 H^+ channel mediates pH-regulated acid secretion by the airway epithelium. These data indicate that apical HVCN1 represents a mechanism to acidify an alkaline airway surface liquid.

The Journal of General Physiology

INTRODUCTION

The pH of the airway surface liquid (ASL) is regulated by several acid and base transporters (for review see Fischer and Widdicombe, 2006). There have been reports of ASL pH values measured in vivo ranging from 5.5 to 8.3, with acidic values found in asthma and cystic fibrosis and alkaline values in rhinitis patients (Fischer and Widdicombe, 2006). Acid secretion by human airways is thought to involve three apical mechanisms: two ATP-dependent transporters (H^+/K^+ ATPase and V-type H^+ ATPase) may transport H^+ against considerable electrochemical H^+ gradients; in contrast, H^+ secretion across H^+ channels requires an outward electrochemical driving force to drive H^+ secretion and open H^+ channels (Cherny et al., 1995). We have previously identified H^+ channels in the apical membrane of human tracheal epithelial cultures and airway cell lines and have found a contribution of apical H^+ channels to acid secretion into the ASL (Fischer et al., 2002).

However, it has been unclear when H^+ channels are physiologically active in airways. Membrane depolarization is a key activator of H^+ channels in phagocytes during the respiratory burst (DeCoursey, 2003b), which depolarize from their resting potential by >100 mV to ~+60 mV (DeCoursey, 2003a). In contrast, the apical membrane potential (V_a) in airways is comparably stable. V_a is determined by the basolateral K^+-dependent potential, which is further depolarized by the apical Cl^- and Na^+ currents to a value of V_a ~−20 mV (Willumsen et al., 1989; Clarke et al., 1992; Willumsen and Boucher, 1992). The activity of the apical Na^+ and Cl^- conductance and the basolateral K^+ conductance regulate V_a. For example, in cystic fibrosis cells, where Cl^- secretion is missing and Na^+ absorption is increased, the apical membrane potential has been shown to be slightly depolarized (by ~10 mV) compared with normal (Willumsen et al., 1989). Compared with phagocytes, this depolarization is quite small, suggesting that the membrane potential in airways has a minor effect on H^+ channel activity. In addition, H^+ channels are sensitively regulated by the H^+ gradient across the plasma membrane (Cherny et al., 1995). Owing to the wide range of measured ASL pH values, it appeared possible that the transmembrane H^+ gradient is the key regulator of H^+ channels in the airways.

Recently, the HVCN1 gene has been identified to code for the plasma membrane H^+ channel (Ramsey et al., 2006; Sasaki et al., 2006). Recombinantly expressed HVCN1 shows many characteristics of the native H^+ channel, including activation by an intra-to-extracellular

Correspondence to Horst Fischer: hfischer@chori.org

Abbreviations used in this paper: ASL, airway surface liquid; GFP, green fluorescent protein; HTE, human primary tracheal epithelial; siRNA, small interfering RNA.

The Rockefeller University Press $30.00
J. Gen. Physiol. Vol. 136 No. 1 35–46
www.jgp.org/cgi/doi/10.1085/jgp.200910379

H^+ gradient, voltage activation, outward rectification, slow time constants of current activation, and block by low micromolar concentrations of Zn^{2+} (DeCoursey, 2003b).

In this study, we asked whether the ASL pH is a factor that regulates airway epithelial H^+ channel–mediated acid secretion, and whether plasma membrane H^+ currents in airway cells are conducted by HVCN1. We found that H^+ channel–mediated acid secretion is activated at a mucosal threshold pH of ~7 and increases with alkalinization of the mucosa. HVCN1 expression was required for H^+ currents by airway cells. During these studies, a novel missense mutation, M91T HVCN1, was identified, which showed a significantly different sensitivity to mucosal pH. The functionally distinct characteristics of this mutation provided additional evidence for the involvement of HVCN1 in airway epithelial acid secretion.

MATERIALS AND METHODS

Cells

The human nasal epithelial cell line JME/CF15 (termed JME here and throughout; Jefferson et al., 1990) was cultured as described in detail previously (Schwarzer et al., 2008). These cells are of cystic fibrosis genotype and express no measurable Cl^- currents under normal conditions. For patch clamping, cells were seeded in small Petri dishes at low density and patch clamped after 1–3 d. Human primary tracheal epithelial (HTE) cultures were provided by the laboratory of J.H. Widdicombe (University of California, Davis, Davis, CA). Use of human tissue was approved by the institutional review board at Children's Hospital & Research Center Oakland. For transepithelial pH stat recordings, HTE and JME cells were cultured on Snapwell filter supports (Corning) as described previously (Fischer et al., 2002). COS-7 cells were provided by T.E. DeCoursey (Rush University Medical Center, Chicago, IL) and cultured as described previously (Morgan et al., 2002).

Measurement of epithelial acid secretion

Acid secretion by confluent epithelial sheets was measured using the pH stat technique in an Ussing chamber as described previously (Cho et al., 2009). Fig. 1 shows a sketch of the orientation of the epithelium in the chamber and the placement of the pH electrode and the titrating burette in the mucosal chamber half. In this study, the serosal pH was stably buffered to pH 7.4, and the mucosal pH was adjusted by titration to target values between 6 and 8. The intracellular pH is not controlled in these measurements. Cultures were mounted in Ussing chambers, and the serosal compartment contained HEPES-buffered solution (composed of [in mM]: 140 NaCl, 12.5 HEPES, 2 KCl, 2 $CaCl_2$, 1 $MgCl_2$, and 5 glucose, pH 7.4, gassed with O_2) and the mucosal compartment contained a buffer-free solution (composed of [in mM]: 145 NaCl, 2 KCl, 2 $CaCl_2$, 1 $MgCl_2$, and 5 glucose, gassed with N_2). The gassing of solutions resulted in a continuous circulation within the compartment. The mucosal pH was measured with a fast-responding electrode (pHC4000-8; Radiometer Analytical) and was continuously titrated with 2 mM NaOH to maintain a constant mucosal pH using a computer-controlled automatic titrator (TIM 865; Radiometer Analytical). Mucosal target pH was increased in steps of ~0.5 pH units (from pH 6 to 8) to determine the rates of acid secretion in dependence of mucosal pH. This was done in the absence and presence of 10 µM $ZnCl_2$ in the mucosal bath to identify the contribution of H^+ channels in these recordings. Recordings were done at 37°C.

Patch clamp recordings

Cells were whole cell patch clamped on the stage of an inverted microscope using an Axopatch 1D amplifier connected to a Digidata 1440A and a Minidigi 1B digitizer. Currents were recorded using PClamp 10 and Axoscope 10 (MDS Analytical Technologies). H^+ currents were measured in solutions that were largely free of small mobile ions. The bath solution contained (in mM): 226 HEPES, 90 TMAOH (trimethylammonium hydroxide), 23 MSA (methanesulfonic acid), 1 $CaCl_2$, and 1 $MgCl_2$, pH 7. Bath solution with pH values between 6 and 8 was prepared by varying the concentrations of HEPES (or MES (2-[*N*-morpholino]ethane sulfonic acid)), TMAOH, and MSA. Bath pH (pH_o) was increased from 6 to 8 by perfusing solutions with increasing pH values into the bath. To control for incomplete washout of the previous solution, pH_o was measured from aliquots taken during experimental runs before perfusion of the next solution. Patch pipettes were filled with solutions made of (in mM): 140 MES or HEPES, 70 or 60 gluconic acid, 90 or 115 TMAOH, 2.5 EGTA, 2 $MgCl_2$, and 1 MgATP, adjusted to pH 6. The bath electrode was filled with the pipette filling solution and was connected to the bath solution through a short agar bridge. The amplifier signal was zeroed before seal formation with the pipette in the bath. In the whole cell recording mode, the membrane potential was continuously clamped to −80 mV and pulsed every 25 s for 6 s to +20 mV to monitor the activation of H^+ currents. Reversal potentials were determined from tail currents exactly as described previously (DeCoursey, 2008). The threshold potential (V_{th}; i.e., the most negative voltage at which H^+ current activated) was determined from depolarizing voltage steps. Recordings were done at room temperature (~20°C).

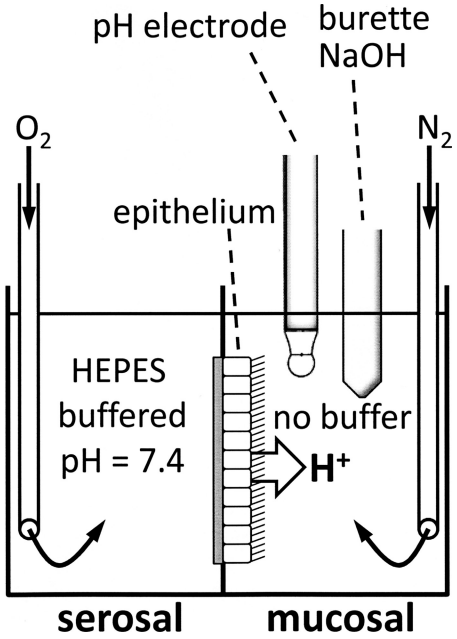

Figure 1. Orientation of epithelium, pH electrode, and titrator burette in Ussing chamber with serosal HEPES-buffered and mucosal unbuffered solutions during pH stat experiments. Solutions were continuously gassed with O_2 (serosally) and N_2 (mucosally) to mix the solutions and prevent air CO_2 from entering.

Small interfering RNA (siRNA)-mediated knockdown of HVCN1 mRNA levels

Using a control green fluorescent protein (GFP) plasmid to probe the efficiency of transfection, we found that JME cells were readily transfected by electroporation (Nucleofector II; Lonza), resulting in transfection of ~90% of cells. Three sets of siRNA (25 mers; Invitrogen) were used that were designed to bind to starting positions 818, 905, and 985 of HVCN1 mRNA (numbering according to GenBank accession no. NM_001040107) and were compared with a control siRNA (Silencer Negative Control siRNA; Applied Biosystems). Two siRNAs resulted in efficient gene knockdown: siRNA818 (5′-gcccggaucaucaaugggauuauca-3′) and siRNA905 (5′-gccgccaagauucaacaccuugagu-3′; one strand given, respectively). Cells were treated with 150 nM siRNA and used after 2–3 d in culture. Determination of HVCN1 mRNA level was done by real-time PCR using an ABI Prism 7000 SDS instrument (Applied Biosystems) and SYBR Green as a reporter. Analysis of HVCN1 mRNA was performed in comparison with GAPDH mRNA using the difference of PCR cycles to reach a threshold amplification (ΔC_T). Probes for HVCN1 were: forward, 5′-catccagcccgacaagaataacta-3′; reverse, 5′-acaatgtcgaggatgaatgaga-3′, resulting in a 183-bp fragment; primers for GAPDH were from Schwarzer et al. (2004). Standard curves were generated for both target and endogenous control genes using serial dilutions of cDNA using 0.4 µM of forward and reverse primers and 50 ng cDNA. To control for specific PCR products, a dissociation curve was generated after the end of the last cycle.

Cloning of HVCN1 from airways

Total RNA was prepared from filter-grown, confluent human primary cultures and reverse transcribed to cDNA. The published HVCN1 cDNA sequence was used as a template to generate gene-specific oligonucleotides (sense, 5′-atggccacctgggacgaaaagg-3′; antisense, 5′-ctagttcacttcaccaagaagtcc-3′). The open reading frame of HVCN1 was amplified, the PCR product was cloned into pCR2.1 vector (TA cloning kit; Invitrogen), and six clones from two different donor tissues were sequenced to full length. Clones were then transferred into a GFP expression vector (pAcGFP-C1; Takara Bio Inc.), the inserted fractions were resequenced, and the resulting plasmids were used to express HVCN1-GFP fusion proteins in COS-7 cells for patch clamp analysis.

Population analysis

The ethnically diverse Coriell genomic DNA SNP500V panel was interrogated for the M91T HVCN1 mutation using a multiplex genotyping system (iPLEX MassARRAY; Sequenom). The following PCR primers, containing a 10-nucleotide 5′ mass tag (underlined) to distinguish them from the probe and extension products (Haff and Smirnov, 1997), were used to amplify a 68-bp fragment containing the HVCN1 polymorphic region: forward, acgttggatgagggccccccttgacttca; reverse, acgttggatgccacctacctgaaacctgtg. The resulting amplified material was subjected to single-nucleotide probe extension using the probe molecule: agctgaacagtttcctcaa. After desalting, the probed material was spotted on a matrix-coated microchip in preparation for MALDI-TOF mass spectrometric analysis (Pusch et al., 2002). MALDI-TOF genotyping results were confirmed by DNA sequencing on a 96 capillary 3730xl DNA Analyzer (Applied Biosystems). The sample was amplified with the following primers containing the forward M13 (18 mer) or the reverse M13 (-24) 16-mer sequencing primer tails (underlined nucleotides) and subjected to Sanger dideoxy capillary electrophoresis DNA sequencing: forward, tgtaaaacgacggccagttaccatgcctggaacatcaa; reverse, aacagctatgaccatgtcatggctcttttctccctg.

Statistics

All data are given as original or as mean ± SE; *n* refers to the number of experiments. Treatment groups were compared by *t* tests or ANOVAs (as described in the text). Relations between reversal potentials, threshold potentials, and pH_o were analyzed by linear regression. $P < 0.05$ was considered significant. All calculations were done with the statistics routines incorporated in Sigmaplot version 11 (Systat Software).

RESULTS

Acid secretion and H^+ currents in airway cells are regulated by the outside pH (pH_o)

Acid secretion into the mucosal medium by JME cultures was investigated using the pH stat technique in Ussing chambers (Fig. 2). Serosal pH was buffered at pH 7.4. Initially, the mucosal pH was allowed to reach an equilibrium pH (pH 6.9 ± 0.05; $n = 5$) at which no acid secretion was apparent. When adjusting the mucosal pH to more alkaline values, epithelial acid secretion increased (Fig. 2 A, filled circles). To identify the H^+ channel–mediated fraction, 10 µM $ZnCl_2$ was added to the mucosal bath (Fig. 2 A, open circles), which blocked acid secretion significantly at pH 7.4 and 8. Fig. 2 B displays the Zn-sensitive fraction of acid secretion (calculated from data in Fig. 2 A). Above a threshold mucosal pH of ~7, Zn-sensitive acid secretion increased at a rate of 339 ± 33.6 nmol × h^{-1} × cm^{-2} per pH unit. This observation suggests that H^+ channel–mediated acid secretion acidifies an alkaline ASL.

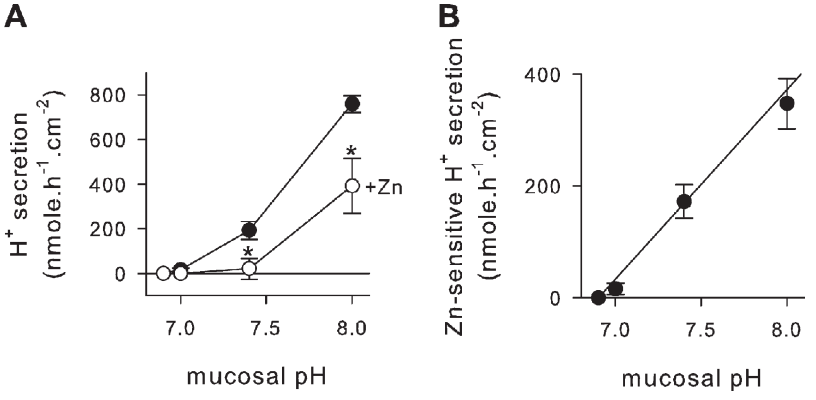

Figure 2. Acid secretion by JME epithelial cultures. (A) Rates of acid secretion in the absence (filled symbols) and presence (open symbols) of 10 µM $ZnCl_2$. Serosal pH 7.4 and mucosal pH was adjusted to 7, 7.4, and 8; $n = 5$. *, significantly different from control; *t* test. (B) Zn-sensitive rates of acid secretion (calculated as the difference from data in A) resulted in an average slope of 339 ± 33.6 nmol × h^{-1} × cm^{-2} × pH^{-1} and a threshold pH of 6.90 (by linear regression).

In the presence of mucosal $ZnCl_2$ (10 μM), a substantial residual acid secretion remained at a mucosal pH of 8 (Fig. 2 A). The non-Zn–sensitive fraction appeared to be driven by the pH gradient. Higher concentrations of $ZnCl_2$ had no additional effects (up to 100 μM nominally); however, owing to the limiting solubility of $Zn(OH)_2$, maximal free Zn^{2+} concentrations in solution are ∼30–40 μM at pH 8 (Cherny and DeCoursey, 1999; Lide, 2000). Whether the residual acid secretion is due to an incompletely blocked H^+ conductance or is carried by other mechanisms was not further investigated here; however, previously it was found that airway epithelia express additional H^+ secretory mechanisms, including an apical bafilomycin-sensitive H^+-ATPase and an apical ouabain-sensitive H^+/K^+-ATPase (Coakley et al., 2003; Inglis et al., 2003; Fischer and Widdicombe, 2006).

These studies in intact epithelia suggested a regulation of the apical H^+ channel by the mucosal pH; however, they do not distinguish between effects on channel activity or effects on driving forces for H^+ exit. This was addressed by investigating the pH dependence of H^+ currents in single JME cells in whole cell patch clamp recordings. Fig. 3 shows patch clamp recordings using pH_o of 6, 7, or 8, and pH_i of 6. H^+ currents were measured during depolarizing pulses as shown in the inset in Fig. 3 A. Measured H^+ currents activated slowly during depolarizing pulses. At an acidic pH_o, currents were small and depolarizations above 40 mV were required for current activation. When pH_o was alkalinized to 7 or 8, H^+ currents increased and activated at lower membrane potentials (Fig. 3, B and C). H^+ currents were fully blocked by 10 μM $ZnCl_2$ added to the bath (Fig. 3 D). Average H^+ current densities for the voltage range of −20 to +80 mV are shown in Fig. 3 E. H^+ currents increased with increasing pH_o and with increasing voltages. Thus, H^+ currents measured in single cells showed qualitatively similar characteristics as epithelial acid secretion, i.e., activation by alkaline pH_o and block by Zn. This suggested that during epithelial acid secretion the H^+ channel was activated by an alkaline mucosal pH. At physiologically expected apical membrane potentials in airways (∼−20 mV), H^+ currents appeared small compared with currents measured at large depolarizing potentials (Fig. 3 E); however, using reasonable estimates to relate epithelial and cellular measurements, the measured H^+ currents could account for epithelial H^+ secretion (see Discussion).

Reversal potentials (E_{rev}) of voltage-activated H^+ currents were determined from tail currents. Examples are

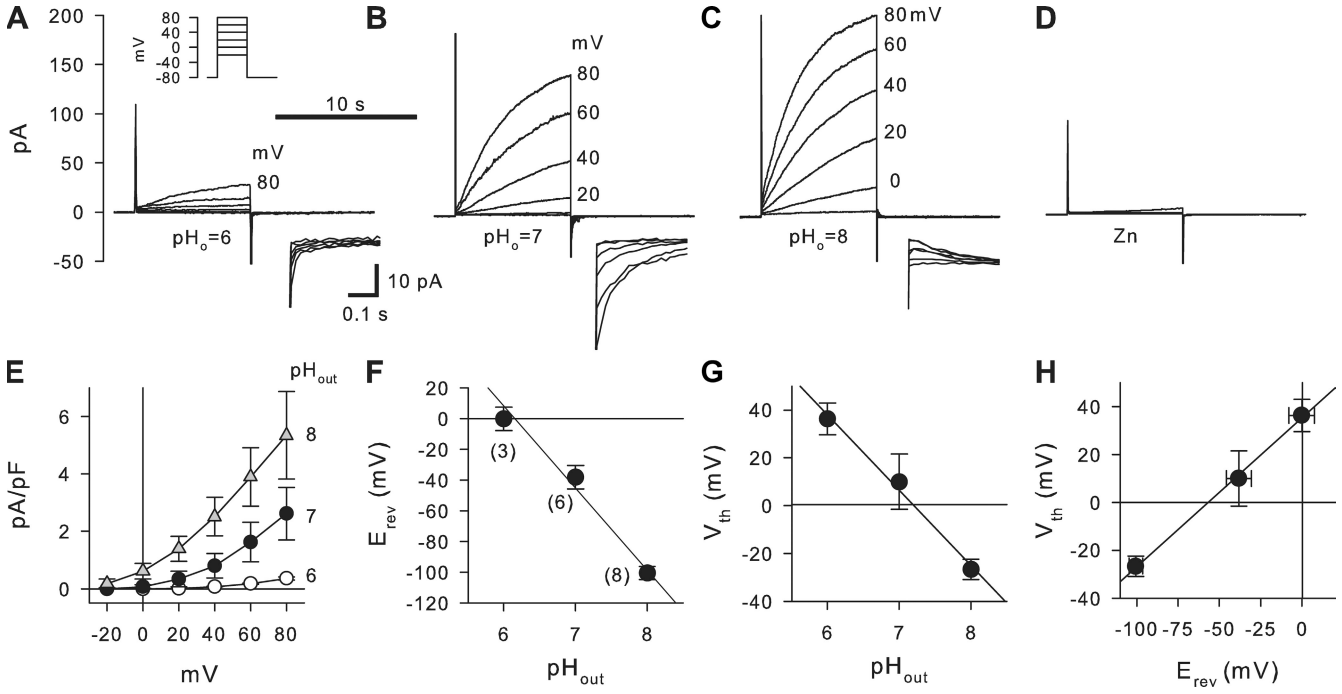

Figure 3. Effect of outside pH (pH_o) on H^+ currents in JME cells. (A–D) Whole cell currents elicited by voltage pulses (as shown in top inset in A) at pH_o 6, 7, and 8 (A–C), and in the presence of 10 μM $ZnCl_2$ at pH_o 8 (D). All recordings are from one cell; pH_i 6. Y axis and 10-s time bar in A are the same for B–D. Selected voltage steps are labeled. The bottom insets in A–C are respective expanded tail currents on a scale as shown in A. (E) Average steady-state current–voltage relations at pH_o 6, 7, and 8 as indicated. Currents were normalized to membrane capacitance. The number of experiments is given in F in parentheses and is the same for E–H. (F) Reversal potential (E_{rev}) was determined from tail currents resulting in a slope of −53 ± 5.1 mV/pH. (G) Threshold potential (V_{th}) as determined from 8-s voltage steps resulted in a slope of −31.5 ± 1.9 mV/pH. (H) Relationship between V_{th} and V_{rev} (using data from F and G) resulted in a slope of 0.62 ± 0.12 mV/mV and an offset of 35.5 ± 7.4 mV.

shown in the insets of Fig. 3 (A–C). E_{rev} was dependent on pH_o (Fig. 3 F) with a slope of −53 ± 5.1 mV/pH, indicating that the applied H^+ gradients in patch clamp recordings were maintained at ∼79% of nominal (using Nernst's equation and assuming perfect selectivity of the H^+ channel; DeCoursey, 2003b). The threshold potentials (V_{th}) and the relation to pH_o and E_{rev} are shown in Fig. 3 (G and H). V_{th} was determined from depolarizing voltage pulses (in 20-mV increments) at pH_o 6, 7, and 8 from recordings as shown in Fig. 3 (A–C) at pH_i 6. Linear regression analysis of the data in Fig. 3 G resulted in a slope of −31.5 ± 1.9 mV/pH. Fig. 3 H shows the relation between threshold potential V_{th} and the reversal potential E_{rev}. Linear regression resulted in a slope of 0.62 ± 0.12 mV/mV and an offset of 35.5 ± 7.4 mV. These data show that increased alkalinization of pH_o or increased outward electrochemical driving forces for H^+ activate H^+ currents in JME cells. To further investigate the role of the HVCN1 H^+ channel in acid secretion, we used molecular approaches that target HVCN1 in measurements of both whole cell H^+ currents and epithelial acid secretion.

HVCN1 expression is required for H^+ currents in airway cells

To determine the role of the HVCN1 H^+ channel in these measurements, we used siRNA to knock down HVCN1 mRNA levels in JME cells and analyzed H^+ currents by whole cell patch clamping. JME cells were transfected by electroporation with one of three siRNAs or a control siRNA (see Materials and methods) and investigated after 2–3 d in culture. Fig. 4 shows the effects of siRNA treatment on levels of HVCN1 mRNA and on H^+ currents. Two of three tested siRNAs resulted in a substantial knockdown of HVCN1 mRNA (siRNA818 and siRNA905) when compared with control treatment (Fig. 4 A). At the same time, in siRNA-treated cells, no voltage-activated currents were measured in the range of applied voltages (Fig. 4 D, inset), and currents were reduced to baseline (Fig. 4, C and D), indicating HVCN1 as the gene responsible for the H^+ currents measured in JME airway cells.

Cloning of HVCN1 from airways and identification of a naturally occurring mutation, M91T

To further investigate the identity of the airway H^+ channel, we cloned the open reading frame of HVCN1 from primary human airway cultures using standard techniques (see Materials and methods). Surprisingly, airway cultures from two different donor tracheas yielded two different HVCN1 clones: one was identical to the published sequence (GenBank accession no. NM_001040107), the other contained two sequential nucleotide variations at positions 437T>C and 438G>A (numbering according to GenBank accession no. NM_001040107), indicating a Met-to-Thr amino acid exchange at codon 91 (M91T) of the HVCN1 protein. To verify these results, we further investigated the occurrence of the M91T mutation in the human population. In 95 genotyped DNA samples of the Coriell genomic DNA SNP500V panel, a single DNA sample (sample NA17172) was identified as heterozygous for the sequential

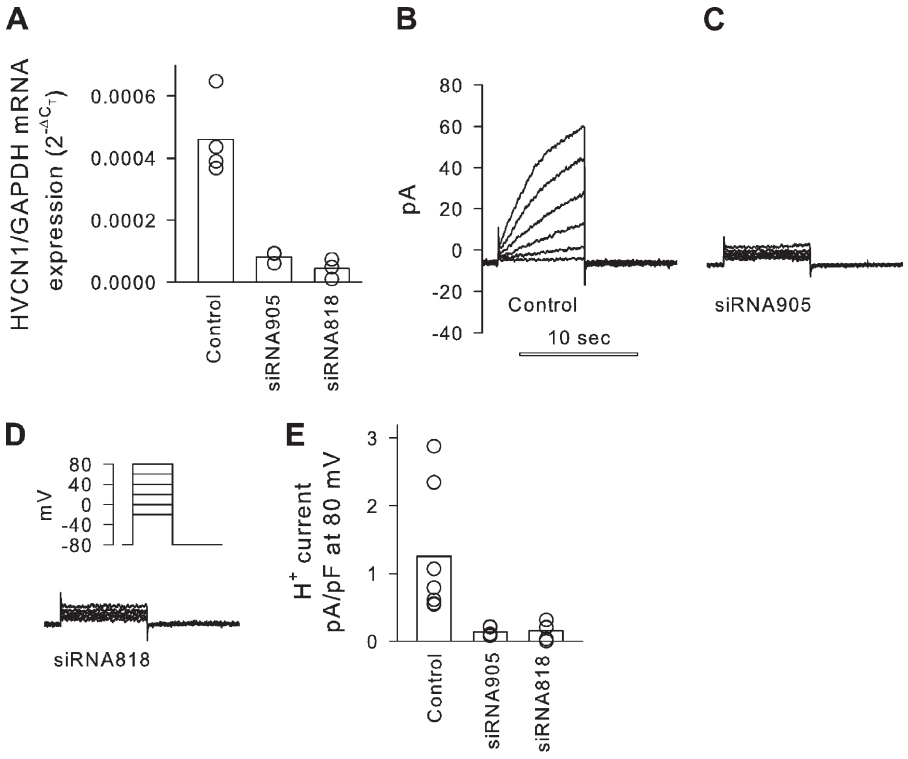

Figure 4. Effect of HVCN1 siRNA on H^+ currents in JME cells. (A) HVCN1 mRNA levels relative to GAPDH mRNA. Treatment with siRNA significantly reduced HVCN1 mRNA levels (P = 0.002; Kruskal-Wallis ANOVA on ranks). Bars, average; symbols, individual measurements. (B–D) H^+ currents measured in single JME cells evoked by depolarizing pulses (as shown in inset); pH_i 6 and pH_o 7. (E) H^+ current density after activation by an 8-s, 80-mV pulse. Treatment with siRNA significantly reduced HVCN1 mRNA levels (P = 0.003; Kruskal-Wallis ANOVA on ranks). Currents measured in siRNA-treated cells were very small (corresponding to a conductance of 79 ± 15 pS/cell) and not voltage activated in the used voltage range.

437T>C/438G>A nucleotide exchanges at codon 91 of HVCN1. The genotyping result was further verified by partial DNA sequencing of this sample, which confirmed the heterozygosity of the mutation. Thus, M91T HVCN1 is a naturally occurring missense mutation that is estimated to occur at a frequency of ~1/190 alleles in the human population.

Epithelial acid secretion of human tracheal cultures expressing wild-type and M91T missense HVCN1

Epithelial acid secretion was measured in primary human airway cultures that were derived from the same tracheal specimens as were used for the cloning of HVCN1; i.e., cultures that expressed endogenous wild-type or M91T HVCN1. As above, as a characteristic of H^+ channel activity, we determined the pH-dependent activation of acid secretion and used 10 µM of mucosal $ZnCl_2$ to block apical H^+ channels. Acid secretion was measured over a range of mucosal pH from 6.0 to 8.0. In cultures that expressed wild-type HVCN1, acid secretion was low at mucosal pH of <7 (Fig. 5 A, filled circles). When mucosal pH was alkalinized to values >7, acid secretion increased steadily. Significant block of acid secretion by $ZnCl_2$ was apparent at alkaline mucosal pH of >7, but not <7. These results closely resembled the results found in JME cells, with the exception that HTE cultures secreted acid at low rates even at quite acidic mucosal pH values of ≤6.5, which is likely related to ATP-driven H^+ secretion in these cells (Fischer et al., 2002; Coakley et al., 2003; Inglis et al., 2003).

Acid secretion by HTE cultures that expressed M91T HVCN1 is shown in Fig. 5 B, and their comparison of the Zn-sensitive acid secretion to wild-type cultures is shown in Fig. 5 C. In contrast to wild-type cultures, M91T HVCN1-expressing cultures showed no Zn-sensitive acid secretion up to a mucosal pH of 7.4 (Fig. 5 B); only at a mucosal pH of 8 was a Zn-sensitive fraction of acid secretion apparent. For comparison, the Zn-sensitive fractions of acid secretion by cultures expressing wild-type and M91T HVCN1 are shown in Fig. 5 C. The threshold pH at which the activation of Zn-sensitive acid secretion was apparent shifted from pH ~7 for wild-type HVCN1-expressing cultures to pH >7.4 in M91T HVCN1-expressing cultures. These observations suggested that the M91T mutation affected the pH sensitivity of Zn-sensitive acid secretion, supporting the notion that HVCN1 is the H^+ channel responsible for acid secretion by airways. To further verify that the difference in acid secretion between the cultures was based on the M91T mutation, we recombinantly expressed wild-type and M91T HVCN1 and characterized the sensitivity of resulting H^+ currents to changes in pH_o.

Patch clamp analysis of recombinantly expressed wild-type and M91T HVCN1

HVCN1 was recombinantly expressed in COS-7 cells. Typical whole cell patch clamp recordings are shown in Fig. 6. Measured H^+ currents in cells recombinantly expressing HVCN1 were considerably larger than currents that were measured in cells that expressed native HVCN1 (compare Figs. 3 and 6). As a result, outward currents during depolarizing pulses showed prominent decays, as discussed in detail previously (DeCoursey and Cherny, 1996; DeCoursey, 2008). This is likely due to an intracellular alkalinization caused by the outward H^+ currents, which limits the quantification of large outward H^+ currents. However, H^+ currents measured around the threshold potential (V_{th}) were likely not affected under the used recording conditions, and thus V_{th} was used in this set of experiments to compare wild-type and M91T HVCN1 activity.

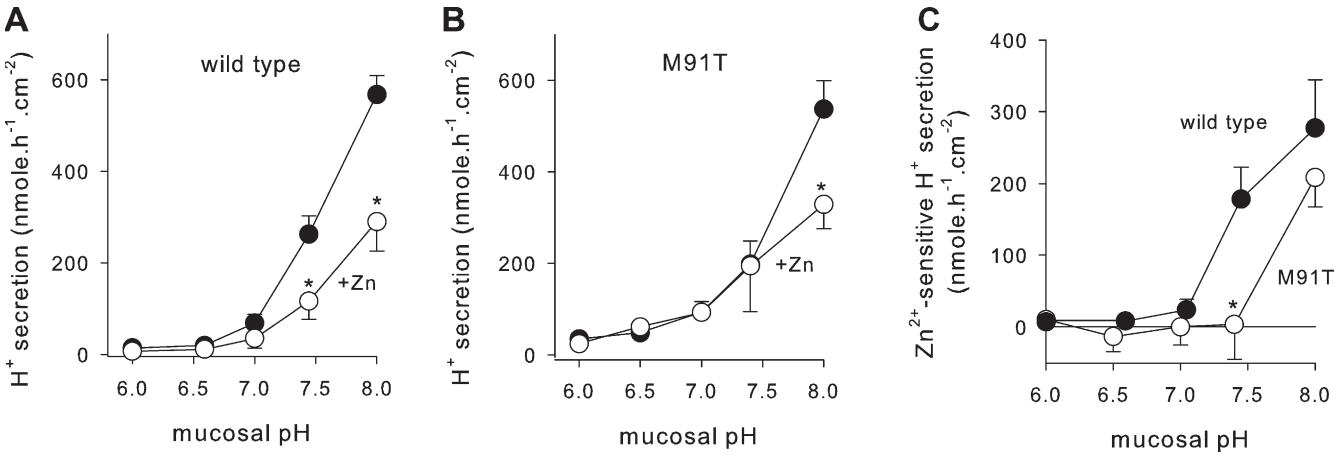

Figure 5. pH dependence of acid secretion of primary human tracheal cultures. Serosal pH 7.4 and mucosal target pH were set to stepwise increasing values over a range of pH 6.0 to 8. (A) Cultures expressing wild-type HVCN1. Filled symbols, untreated; open symbols, 10 µM $ZnCl_2$ mucosally. (B) Primary human tracheal cultures expressing M91T HVCN1. (C) Activation of Zn-sensitive acid secretion by mucosal alkalinization in wild-type (filled symbols) and M91T HVCN1 (open symbols). Data were calculated as the difference of values before-minus-after Zn addition from data in A and B. *, significantly different from control; *t* test.

Fig. 6 A shows an overview recording of the typical protocol used to investigate the voltage-dependent activation and Zn sensitivity of recombinantly expressed HVCN1. The membrane potential (Fig. 6 A, bottom tracing) was held at −80 mV and pulsed to 20 mV every 40 s to monitor the activation of H^+ currents. Voltage step protocols were applied before and after the addition of 10 μM $ZnCl_2$ to the bath. Fig. 6 (B–J) shows recordings that were obtained from cells that expressed recombinant wild-type HVCN1 (Fig. 6, B–D) or M91T HVCN1 (Fig. 6, E–G), or were from mock-transfected cells (Fig. 6, H–J). Recombinant expression of wild-type or M91T HVCN1 resulted in typical, slowly depolarization-activated H^+ currents. In the presence of a nominal

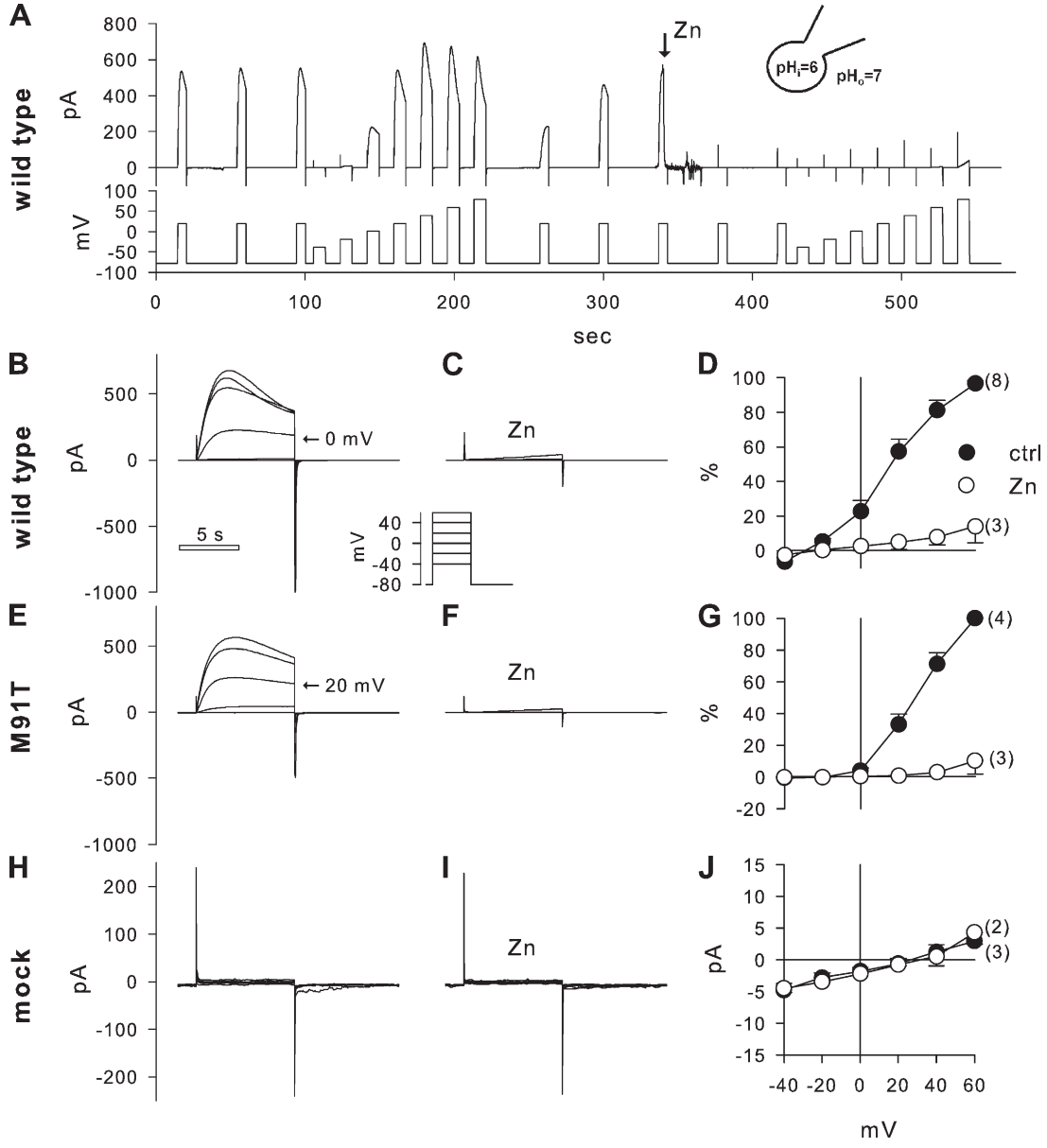

Figure 6. Patch clamp recordings of H^+ currents after recombinant expression of wild-type HVCN1, M91T HVCN1, and empty vector in COS-7 cells. (A) Typical overview recording for this set of experiments. Top trace shows current measured at holding potentials as shown in the bottom trace. Baseline voltage was −80 mV, pulsed every 40 s to +20 mV, and a voltage step protocol from −40 to +80 mV, step 20 mV, was applied before and after 10 μM $ZnCl_2$ was added to the bath; pH_i 6 and pH_o 7. Note the recovery of depolarization-activated currents after the first current–voltage steps. (B–D) Recording from cells expressing recombinant wild-type HVCN1. Current pulse to 0 mV is indicated in B, and voltage step protocol is depicted in the inset; recordings in B and C are from the same cell, and the y-axis scaling is the same. (E–G) Recording from a cell expressing recombinant M91T HVCN1. Current pulse at 20 mV is indicated in E; recordings in E and F are from the same cell, and the y-axis scaling is the same. (H–J) Mock-transfected cells expressed no significant currents. The y axis in I is the same as in H. The time bar in B is the same for all current recordings (excluding A). Recordings in H and I are from the same cell, and the y-axis scaling is the same. D and G are reported in percent of maximal current, and the x axis is the same as in J. The number of experiments is given in parentheses.

1-pH gradient (pH_i 6 and pH_o 7), H^+ currents carried by wild-type HVCN1 activated at potentials larger than −20 mV. In contrast, M91T HVCN1 appeared less sensitive to depolarizing voltage pulses and required higher voltages for current activation, which resulted in a shift of the current–voltage relation of M91T HVCN1 to the right compared with wild type (compare Fig. 6, D with G), suggesting that the M91T mutation affects HVCN1 activation. Both wild-type and M91T HVCN1 were readily blocked by 10 μM $ZnCl_2$ (Fig. 6, C and F). Mock-transfected COS-7 cells showed no measurable currents and no effect of $ZnCl_2$ (Fig. 6, H–J).

The pH dependence of recombinantly expressed wild-type or M91T HVCN1 was determined from threshold potentials (V_{th}) of H^+ currents over a pH_o range of ∼6 to 8. V_{th} was previously shown to be strongly pH dependent (Cherny and DeCoursey, 1999). V_{th} was determined from depolarizing voltage pulses from a baseline potential of −80 mV. Fig. 7 shows examples of current recordings evoked by voltage pulses near V_{th} from wild-type (Fig. 7, A and C) and M91T HVCN1-transfected COS-7 cells (Fig. 7, B and D) using pH_i 6 and pH_o as stated in the figures. At pH_o 7.1, wild-type HVCN1 was typically activated by pulses to −20 mV (Fig. 7 A), whereas M91T HVCN1 required a depolarization to 0 mV (Fig. 7 B) for current activation. A more alkaline pH_o (Fig. 7, C and D) resulted in current activation at lower potentials for both HVCN1 constructs; however, M91T HVCN1-mediated currents consistently required ∼20 mV stronger depolarizations than wild-type HVCN1 for current activation. Fig. 7 E shows average V_{th} at pH_i 6 for wild type (open symbols) and M91T HVCN1 (filled symbols). The slope of these plots was not affected by the M91T mutation (wild type, −28.1 ± 3.6 mV/pH; M91T, −30.3 ± 3.1 mV/pH); however, the M91T mutation caused a significant right-shift of V_{th} to higher pH_o values by 0.65 pH units (at V_{th} 0: wild type, 6.43 ± 0.08; M91T, 7.08 ± 0.05; $P < 0.001$), suggesting that larger H^+ gradients are required for the activation of M91T HVCN1. The corresponding relationship between V_{th} and E_{rev} is shown in Fig. 7 F. Linear regression analysis of these data resulted in similar slopes of 0.78 ± 0.06 mV/mV (wild type) and 0.81 ± 0.09 mV/mV (M91T, NS), but M91T showed a significantly higher offset of 34.4 ± 4.7 mV compared with wild type (2.1 ± 1.9 mV; $P < 0.001$), indicating that M91T HVCN1 required comparably larger pH gradients for H^+ current activation.

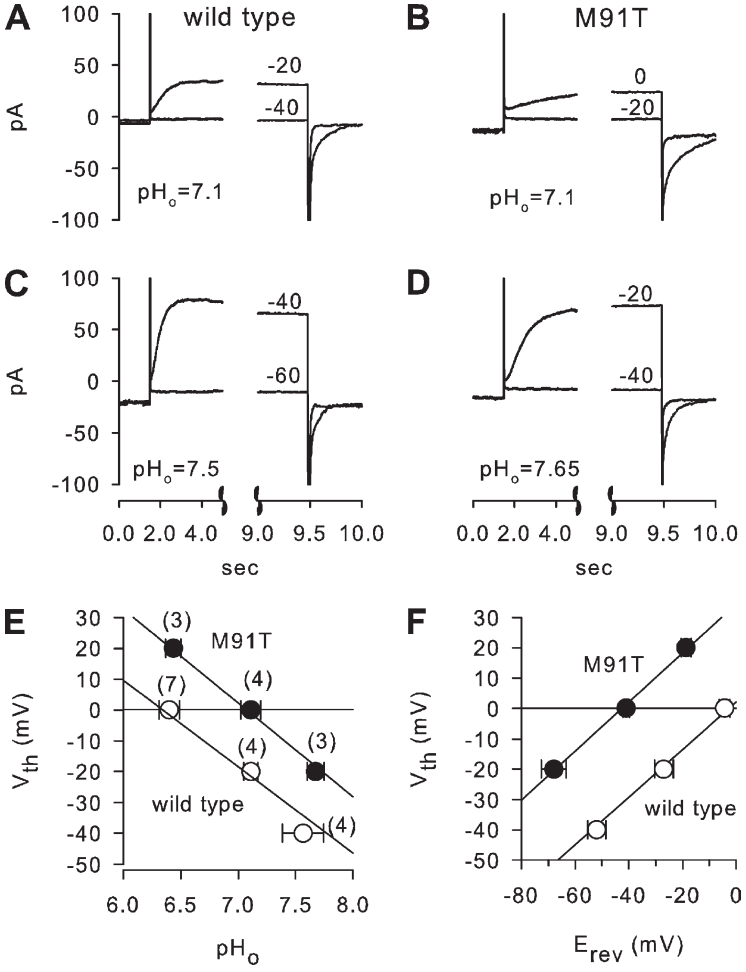

Figure 7. Threshold potentials of H^+ current activation across recombinantly expressed wild-type and M91T HVCN1 in COS-7 cells. (A and C) Wild-type HVCN1. Example recordings of depolarizing steps from −80 mV to potentials near V_{th} at pH_o 7.1 (A) and 7.5 (B) from one cell. Clamped voltages are given next to traces. Tail currents are shown on an expanded time scale (note the break in time axes); pH_i 6. (B and D) Corresponding recording from an M91T HVCN1 at pH_o 7.1 (B) and 7.65 (D) recorded from same cell; pH_i 6. pH_o was determined from aliquots taken from bath solution for every condition during experimental runs. (E) Relationship between V_{th} and pH_o. Linear regression analysis for wild-type and M91T resulted in similar slopes of wild type (−28.1 ± 3.6 mV/pH_o) and M91T (−30.3 ± 3.1 mV/pH_o). Correspondingly, M91T required significantly higher pH_o (7.08 ± 0.05) than wild type (6.43 ± 0.08; $P < 0.001$). The number of experiments is given in parentheses. (F) Relationship between V_{th} and E_{rev} for wild-type and M91T HVCN1. Regression analysis yielded the following: wild-type, $V_{th} = 0.78 \pm 0.06\ E_{rev} + 2.1 \pm 1.9$ mV; M91T, $V_{th} = 0.81 \pm 0.09\ E_{rev} + 34 \pm 4.7$ mV. Offset, but not slope, was significantly different ($P < 0.001$; *t* tests).

Previously, it was noted that recombinantly expressed HVCN1 activates at significantly lower membrane potentials than native H^+ channels (Musset et al., 2008). This is also apparent in the current study when comparing native H^+ currents in JME cells with recombinantly expressed HVCN1 in COS-7 cells (compare Figs. 3, G and H, and 7, E and F). Threshold potentials of H^+ currents across recombinant HVCN1 were shifted by −33 mV compared with native H^+ currents in JME cells (compare Figs. 3 H and 7 F). Correspondingly, recombinant HVCN1 activated at ∼0.7 pH units more acidic pH_o than native HVCN1 (compare Figs. 3 G and 7 E). Despite this difference between native and recombinant HVCN1 H^+ currents, the recordings of recombinant wild-type and M91T HVCN1 show a significant effect of the M91T mutation on pH-dependent current activation; i.e., M91T HVCN1 forms an H^+ channel with an altered pH sensitivity that would be expected to show reduced activity in airways. The similar pH-dependent behavior of M91T HVCN1 H^+ currents and epithelial acid secretion by M91T HVCN1-expressing cultures suggests that HVCN1 is the H^+ channel responsible for acid secretion by airways.

DISCUSSION

Zn-sensitive acid secretion has been shown in airway epithelial tissues, primary cultures, or cell lines, and H^+ channel activity has been found in single airway cells (Fischer et al., 2002; Schwarzer et al., 2004; Cho et al., 2009). Similar to H^+ currents studied in other cell types, H^+ currents measured in airways were activated by an outward electrochemical H^+ gradient. Based on previous measurements of the apical membrane potential of ∼−20 mV in airway epithelia (Willumsen and Boucher, 1989; Clarke et al., 1992; Willumsen and Boucher, 1992), and the functional characteristics of the H^+ channel, it was not clear when the H^+ channel is active in the apical membrane. Also, measurements of pH_i in airway cells of ∼7.1 (Willumsen and Boucher, 1992; Paradiso, 1997; Paradiso et al., 2003) and ASL pH of <7 (Kyle et al., 1990; Jayaraman et al., 2001a,b) suggested that electrochemical gradients for H^+ across the apical membrane are inward, which would keep H^+ channels closed (DeCoursey, 2003b). The mismatch of the observed characteristics of epithelial acid secretion and the described functional characteristics of the H^+ channel was puzzling and was the basis for this study.

Evidence that HVCN1 mediates acid secretion by airways

This study provides several lines of evidence that the HVCN1 H^+ channel contributes to epithelial acid secretion in a pH-dependent manner. These are based on block by Zn^{2+}, functional characteristics, and the properties of the newly identified missense mutation, M91T HVCN1.

Block by Zn^{2+}. The HVCN1 H^+ channel is blocked by low micromolar concentrations of $ZnCl_2$. For example, Ramsey et al. (2006) recently found HVCN1 to be blocked by $ZnCl_2$ at a half-maximal effective concentration of 1.9 µM. In the current report, we readily blocked H^+ currents in whole cell patch clamp recordings and transepithelial acid secretion in both JME and primary HTE cultures using 10 µM $ZnCl_2$ (compare Figs. 2, 3 D, and 5). The consistent block of acid secretion and H^+ currents in this study, and of both native H^+ currents and HVCN1 in many previous studies (Cherny and DeCoursey, 1999; DeCoursey, 2003b; Ramsey et al., 2006), is one functional indication for HVCN1 H^+ currents in epithelial acid secretion.

Rectification of acid secretion. In whole cell recordings, H^+ currents rectify strongly based on the voltage-dependent characteristics of the channel, but more importantly for epithelial function, based on the required inside-to-outside H^+ gradient. These functional characteristics result in H^+ being conducted only outwards (DeCoursey, 2008). In epithelial recordings, we similarly observed a strong rectification of acid secretion, which was always directed toward the mucosa. In both JME and HTE, acid secretion was apparent only above a mucosal threshold pH of ∼7 (compare Figs. 2 A and 5 A). In HTE, we found no noticeable reversal at acidic mucosal pH levels down to 6. Thus, epithelial acid secretion shows strong rectification, similar to the pH-dependent characteristics of the H^+ channel in whole cell recordings.

Activation by mucosal alkalinity. H^+ currents have been described to activate in the presence of an inside-to-outside H^+ gradient (Cherny et al., 1995). Because of reports that the ASL pH varies over a wide range (Fischer and Widdicombe, 2006), an effect on the apical H^+ conductance could be expected. In this study, we used the pH dependence as another functional characteristic to identify the role of H^+ channels during epithelial acid secretion. We found that acid secretion was activated by mucosal alkalinity above a threshold pH of ∼7 in both JME and HTE cells. Similarly, whole cell H^+ currents in JME cells were activated pH-dependently by alkaline pH_o values, although currents appeared quite small at physiological potentials. However, when quantitatively comparing the transepithelial and patch clamp data, the measurements appear to coincide reasonably: when (a) considering Zn-sensitive acid secretion by JME cells at a mucosal pH of 8 of 347 nmol × h^{-1} × cm^{-2} (Fig. 2 B, corresponding to 9.4 µA/cm^2) and (b) assuming an apical capacitance of 3 µF/cm^2 (Danahay et al., 2006), and (c) a ratio between apical and basolateral membrane capacitance of 1:10 (Danahay et al., 2006), an H^+ current of ∼0.31 pA/pF is predicted from the measured epithelial acid secretion for a corresponding whole cell patch clamp measurement. For comparison, we observed

whole cell H^+ currents of 0.18 pA/pF (at a pH_o 8, membrane potential of −20 mV, and nominal pH_i of 6; Fig. 3 E). The roughly twofold overestimation of whole cell H^+ currents from acid secretion may be explained by (a) the unknown apical membrane potential and pH_i in JME epithelia during the pH stat recordings, (b) the temperature dependence of H^+ channel activity (Kuno et al., 1997; DeCoursey and Cherny, 1998) and the difference in temperature used in this study in epithelial (37°C) and patch clamp measurements (∼20°C), and (c) the somewhat reduced H^+ gradients across the membrane (to ∼79% of nominal; Fig. 3 F). This estimation suggests that the measured whole cell H^+ channel activity could account for the measured epithelial acid secretion.

Knockdown of HVCN1 expression reduces H^+ currents. We used siRNA to knock down the levels of HVCN1 mRNA. The JME cell line was advantageous because it was the only airway epithelial cell type that, in our hands, allowed for an efficient transfection with siRNA. On average, levels of HVCN1 mRNA were reduced to ∼13% by siRNA treatment, and, at the same time, H^+ currents measured in single cells were reduced to baseline (Fig. 4). In our study, we have investigated a limited voltage range up to 80 mV. We cannot exclude that at higher voltages the HVCN1 mRNA levels remaining after knockdown could generate measurable H^+ currents, which could be expected from the strong voltage dependence of H^+ currents (DeCoursey, 2008). Nevertheless, concurrent knockdown of HVCN1 mRNA and H^+ channel function indicates HVCN1 in whole cell H^+ currents in airway cells.

The functional characteristics of the M91T HVCN1 mutation are found in epithelial acid secretion. The M91T HVCN1 mutation showed distinct H^+ channel activation, such that 0.65 pH units more alkaline pH_o was required for current activation at any membrane potential investigated (Fig. 7 E). This functional characteristic of M91T HVCN1 was also found in epithelial cultures that natively expressed this mutation. Acid secretion by these cultures showed a mucosal threshold pH that was ∼0.5 pH units more alkaline than in wild-type cultures (Fig. 5 C). Thus, the phenotype of M91T HVCN1 served here as a molecular tool to identify HVCN1 function in acid secretion by epithelial preparations.

pH dependence of acid secretion by airways

In previous measurements of the ASL pH of epithelial cultures or in animal models under controlled conditions, the average ASL pH was found to be ∼6.9 (Kyle et al., 1990; Jayaraman et al., 2001a,b). Our current data suggest that at ASL pH 6.9, acid secretion is low and the H^+ channel is likely closed. However, ASL pH has been found to alkalinize to values >7 (Fischer and Widdicombe, 2006), and extremes of >8 have been measured under certain conditions (England et al., 1999; Paget-Brown et al., 2007). Although the reason for an excessive alkalinization of the airways is not fully understood, it may be governed by CFTR-mediated HCO_3^- secretion into the ASL (Ballard et al., 1999; Thiagarajah et al., 2004). Our data suggest that above a threshold pH of 7, H^+ channels and acid secretion are activated, which would re-acidify an alkaline ASL. Thus, we suggest that the function of the apical HVCN1 H^+ channel in airways is to acidify and maintain the mucosal pH under conditions of base secretion.

Owing to the reported range of ASL pH values, this study largely focused on the effects of pH_o on H^+ channel function. However, the pH gradient across the membrane, rather than the absolute pH value, determines H^+ channel activity (Cherny et al., 1995). Therefore, intracellular acidification may similarly drive acid secretion across H^+ channels. For example, we recently identified an apocyanin-sensitive intracellular acid production that was likely based on the NADPH oxidase DUOX that is localized in the apical membrane in HTE cells (Schwarzer et al., 2004). Our current study suggests that apical H^+ channels release intracellularly produced acid across the apical membrane, driven by a cell-to-ASL H^+ gradient.

Characteristics of M91T HVCN1

An unexpected finding during this study was the identification of, to our knowledge, the first naturally occurring missense mutation described in HVCN1. In wild-type HVCN1, M91 is located in the intracellular N-terminal tail just before the first transmembrane-spanning domain. There are no known functions of this part of the channel. Recently, a putative phosphorylation site at the

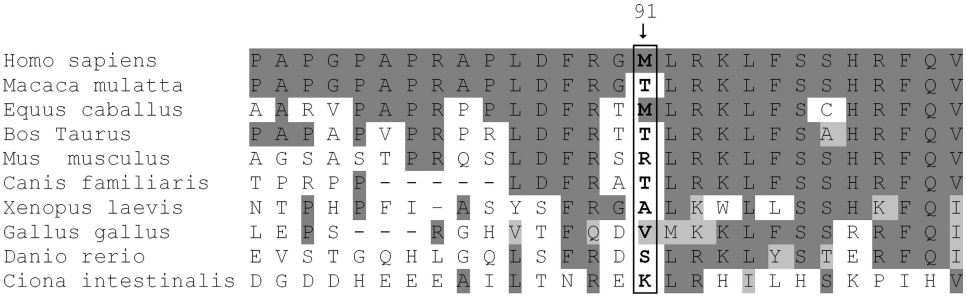

Figure 8. Alignment of the HVCN1 region around M91 for several species. Position 91 is boxed. Identical residues are marked dark gray, and similar residues are marked light gray. Alignment with the human sequence was done using BlastP (http://blast.ncbi.nlm.nih.gov).

nearby position S97 was shown to be phosphorylated in vitro, but recombinantly expressed S97A HVCN1 resulted in normal H^+ channel activity (Musset et al., 2010). Because neither the M91 nor the T91 residue is likely to participate in H^+ binding, the mutation may introduce structural changes that interfere with the sites that sense the H^+ gradient. These H^+-sensing sites of HVCN1 are not known (DeCoursey, 2008). Previously, it has been proposed that protonation of extracellular site(s) maintains the closed state and protonation of intracellular site(s) maintains the open state of the channel; however, how the M91 site relates to these putative sites is unclear.

Fig. 8 shows an alignment of HVCN1 of the region around the M91 site for 10 species. In general, the N-terminal tail shows little conservation between species (Sasaki et al., 2006), M91 does not appear to be conserved even in closely related species, and T91 is a common residue in the species listed in Fig. 8. Residue 91 is a methionine in human and horse, but a threonine in rhesus monkey, cow, and dog. Interestingly, the rhesus monkey HVCN1 expresses T91 and is otherwise very similar to the human sequence (92% identical and 95% similar).

Our study focused largely on the function of the HVCN1 H^+ channel in the airways; however, the cell types with the highest HVCN1 expression are phagocytes (Ramsey et al., 2006), and a mutation in HVCN1 could be expected to affect the phagocytic innate defense function. However, the tissue sample that expressed the M91T mutation was obtained from an 84-yr-old donor (cause of death unknown) with an uneventful medical history and no recorded indications for increased disease susceptibility, airway conditions, or any other conspicuous ailment.

The measurements shown in Fig. 5 B on primary cultures that express the M91T HVCN1 mutation were likely of heterozygous wild-type/M91T genotype. This is based on the observed frequency of the M91T mutation of 1 in 95 samples in the human population, which makes a homozygous M91T genotype unlikely (~1 in 36,000), although we were not able to confirm heterozygosity in this sample used for the studies shown in Fig. 5 B. Previously, it was found that recombinantly expressed HVCN1 forms functional homodimers of two HVCN1 subunits in the plasma membrane with two separate conduction pathways (Koch et al., 2008; Lee et al., 2008; Tombola et al., 2008). Our measurements showed a prominent change in function of acid secretion in tissues that expressed M91T HVCN1. When assuming heterozygosity of the sample, this observation suggests that either the M91T mutant is expressed in a dominant fashion and forms M91T/M91T dimers with altered function, or both alleles are expressed, resulting in a mixture of M91T and wild-type homodimers and heterodimers, whose summary function shows altered pH sensitivity. These cases cannot be distinguished based on the data of this study but highlight the possibilities to be encountered when investigating native HVCN1 mutants.

In conclusion, this study provides indications that the apical HVCN1 H^+ channel contributes to airway epithelial acid secretion at an ASL pH >7. We suggest that, in contrast to H^+ channels in phagocytes, the physiological mechanism of activation of the airway H^+ channel uses the pH gradient rather than membrane depolarization, and thus may operate under conditions where its open probability is quite low. Several H^+ channel characteristics, including the altered pH sensitivity of the M91T HVCN1 H^+ channel, were found in epithelial recordings implicating HVCN1 in airway epithelial acid secretion.

We thank Marrah E. Lachowicz-Scroggins and Dr. Jonathan H. Widdicombe (University of California, Davis) for primary airway cell cultures and Mohammad Hajighasemi for assistance with pH stat experiments. Dr. Miklos Geiszt (Semmelweis University, Budapest, Hungary) kindly provided an HVCN1 clone for studies that led up to this project.

This study was supported in part by the National Institutes of Health (grants R21 HL089196 and R01 HL086323) and the Cystic Fibrosis Foundation (grant FISCHE07G0).

Christopher Miller served as editor.

Submitted: 9 December 2009
Accepted: 26 May 2010

REFERENCES

Ballard, S.T., L. Trout, Z. Bebök, E.J. Sorscher, and A. Crews. 1999. CFTR involvement in chloride, bicarbonate, and liquid secretion by airway submucosal glands. *Am. J. Physiol.* 277:L694–L699.

Cherny, V.V., and T.E. DeCoursey. 1999. pH-dependent inhibition of voltage-gated H^+ currents in rat alveolar epithelial cells by Zn^{2+} and other divalent cations. *J. Gen. Physiol.* 114:819–838. doi:10.1085/jgp.114.6.819

Cherny, V.V., V.S. Markin, and T.E. DeCoursey. 1995. The voltage-activated hydrogen ion conductance in rat alveolar epithelial cells is determined by the pH gradient. *J. Gen. Physiol.* 105:861–896. doi:10.1085/jgp.105.6.861

Cho, D.Y., M. Hajighasemi, P.H. Hwang, B. Illek, and H. Fischer. 2009. Proton secretion in freshly excised sinonasal mucosa from asthma and sinusitis patients. *Am. J. Rhinol. Allergy.* 23:e10–e13. doi:10.2500/ajra.2009.23.3389

Clarke, L.L., A.M. Paradiso, and R.C. Boucher. 1992. Histamine-induced Cl^- secretion in human nasal epithelium: responses of apical and basolateral membranes. *Am. J. Physiol.* 263:C1190–C1199.

Coakley, R.D., B.R. Grubb, A.M. Paradiso, J.T. Gatzy, L.G. Johnson, S.M. Kreda, W.K. O'Neal, and R.C. Boucher. 2003. Abnormal surface liquid pH regulation by cultured cystic fibrosis bronchial epithelium. *Proc. Natl. Acad. Sci. USA.* 100:16083–16088. doi:10.1073/pnas.2634339100

Danahay, H., H.C. Atherton, A.D. Jackson, J.L. Kreindler, C.T. Poll, and R.J. Bridges. 2006. Membrane capacitance and conductance changes parallel mucin secretion in the human airway epithelium. *Am. J. Physiol. Lung Cell. Mol. Physiol.* 290:L558–L569. doi:10.1152/ajplung.00351.2005

DeCoursey, T.E. 2003a. Interactions between NADPH oxidase and voltage-gated proton channels: why electron transport depends on proton transport. *FEBS Lett.* 555:57–61. doi:10.1016/S0014-5793(03)01103-7

DeCoursey, T.E. 2003b. Voltage-gated proton channels and other proton transfer pathways. *Physiol. Rev.* 83:475–579.

DeCoursey, T.E. 2008. Voltage-gated proton channels: what's next? *J. Physiol.* 586:5305–5324. doi:10.1113/jphysiol.2008.161703

DeCoursey, T.E., and V.V. Cherny. 1996. Effects of buffer concentration on voltage-gated H^+ currents: does diffusion limit the conductance? *Biophys. J.* 71:182–193. doi:10.1016/S0006-3495(96)79215-9

DeCoursey, T.E., and V.V. Cherny. 1998. Temperature dependence of voltage-gated H^+ currents in human neutrophils, rat alveolar epithelial cells, and mammalian phagocytes. *J. Gen. Physiol.* 112:503–522. doi:10.1085/jgp.112.4.503

England, R.J., J.J. Homer, L.C. Knight, and S.R. Ell. 1999. Nasal pH measurement: a reliable and repeatable parameter. *Clin. Otolaryngol. Allied Sci.* 24:67–68. doi:10.1046/j.1365-2273.1999.00223.x

Fischer, H., and J.H. Widdicombe. 2006. Mechanisms of acid and base secretion by the airway epithelium. *J. Membr. Biol.* 211:139–150. doi:10.1007/s00232-006-0861-0

Fischer, H., J.H. Widdicombe, and B. Illek. 2002. Acid secretion and proton conductance in human airway epithelium. *Am. J. Physiol. Cell Physiol.* 282:C736–C743.

Haff, L.A., and I.P. Smirnov. 1997. Multiplex genotyping of PCR products with MassTag-labeled primers. *Nucleic Acids Res.* 25:3749–3750. doi:10.1093/nar/25.18.3749

Inglis, S.K., S.M. Wilson, and R.E. Olver. 2003. Secretion of acid and base equivalents by intact distal airways. *Am. J. Physiol. Lung Cell. Mol. Physiol.* 284:L855–L862.

Jayaraman, S., Y. Song, and A.S. Verkman. 2001a. Airway surface liquid pH in well-differentiated airway epithelial cell cultures and mouse trachea. *Am. J. Physiol. Cell Physiol.* 281:C1504–C1511.

Jayaraman, S., Y. Song, L. Vetrivel, L. Shankar, and A.S. Verkman. 2001b. Noninvasive in vivo fluorescence measurement of airway-surface liquid depth, salt concentration, and pH. *J. Clin. Invest.* 107:317–324. doi:10.1172/JCI11154

Jefferson, D.M., J.D. Valentich, F.C. Marini, S.A. Grubman, M.C. Iannuzzi, H.L. Dorkin, M. Li, K.W. Klinger, and M.J. Welsh. 1990. Expression of normal and cystic fibrosis phenotypes by continuous airway epithelial cell lines. *Am. J. Physiol.* 259:L496–L505.

Koch, H.P., T. Kurokawa, Y. Okochi, M. Sasaki, Y. Okamura, and H.P. Larsson. 2008. Multimeric nature of voltage-gated proton channels. *Proc. Natl. Acad. Sci. USA.* 105:9111–9116. doi:10.1073/pnas.0801553105

Kuno, M., J. Kawawaki, and F. Nakamura. 1997. A highly temperature-sensitive proton current in mouse bone marrow–derived mast cells. *J. Gen. Physiol.* 109:731–740. doi:10.1085/jgp.109.6.731

Kyle, H., J.P. Ward, and J.G. Widdicombe. 1990. Control of pH of airway surface liquid of the ferret trachea in vitro. *J. Appl. Physiol.* 68:135–140.

Lee, S.-Y., J.A. Letts, and R. Mackinnon. 2008. Dimeric subunit stoichiometry of the human voltage-dependent proton channel Hv1. *Proc. Natl. Acad. Sci. USA.* 105:7692–7695. doi:10.1073/pnas.0803277105

Lide, D.R., editor. 2000. Handbook of Chemistry and Physics. 81st edition. CRC Press, Boca Raton, FL. 2556 pp.

Morgan, D., V.V. Cherny, M.O. Price, M.C. Dinauer, and T.E. DeCoursey. 2002. Absence of proton channels in COS-7 cells expressing functional NADPH oxidase components. *J. Gen. Physiol.* 119:571–580. doi:10.1085/jgp.20018544

Musset, B., V.V. Cherny, D. Morgan, Y. Okamura, I.S. Ramsey, D.E. Clapham, and T.E. DeCoursey. 2008. Detailed comparison of expressed and native voltage-gated proton channel currents. *J. Physiol.* 586:2477–2486. doi:10.1113/jphysiol.2007.149427

Musset, B., M. Capasso, V.V. Cherny, D. Morgan, M. Bhamrah, M.J.S. Dyer, and T.E. DeCoursey. 2010. Identification of Thr29 as a critical phosphorylation site that activates the human proton channel Hvcn1 in leukocytes. *J. Biol. Chem.* 285:5117–5121. doi:10.1074/jbc.C109.082727

Paget-Brown, A.O., J.F. Hunt, and B. Gaston. 2007. Tracheal aspirate pH is alkaline in pre-term human infants. *Eur. Respir. J.* 30:840–842. doi:10.1183/09031936.00015507

Paradiso, A.M. 1997. ATP-activated basolateral Na^+/H^+ exchange in human normal and cystic fibrosis airway epithelium. *Am. J. Physiol.* 273:L148–L158.

Paradiso, A.M., R.D. Coakley, and R.C. Boucher. 2003. Polarized distribution of HCO3− transport in human normal and cystic fibrosis nasal epithelia. *J. Physiol.* 548:203–218. doi:10.1113/jphysiol.2002.034447

Pusch, W., J.H. Wurmbach, H. Thiele, and M. Kostrzewa. 2002. MALDI-TOF mass spectrometry-based SNP genotyping. *Pharmacogenomics.* 3:537–548. doi:10.1517/14622416.3.4.537

Ramsey, I.S., M.M. Moran, J.A. Chong, and D.E. Clapham. 2006. A voltage-gated proton-selective channel lacking the pore domain. *Nature.* 440:1213–1216. doi:10.1038/nature04700

Sasaki, M., M. Takagi, and Y. Okamura. 2006. A voltage sensor-domain protein is a voltage-gated proton channel. *Science.* 312:589–592. doi:10.1126/science.1122352

Schwarzer, C., T.E. Machen, B. Illek, and H. Fischer. 2004. NADPH oxidase-dependent acid production in airway epithelial cells. *J. Biol. Chem.* 279:36454–36461. doi:10.1074/jbc.M404983200

Schwarzer, C., Z. Fu, H. Fischer, and T.E. Machen. 2008. Redox-independent activation of NF-kappaB by Pseudomonas aeruginosa pyocyanin in a cystic fibrosis airway epithelial cell line. *J. Biol. Chem.* 283:27144–27153. doi:10.1074/jbc.M709693200

Thiagarajah, J.R., Y. Song, P.M. Haggie, and A.S. Verkman. 2004. A small molecule CFTR inhibitor produces cystic fibrosis-like submucosal gland fluid secretions in normal airways. *FASEB J.* 18:875–877.

Tombola, F., M.H. Ulbrich, and E.Y. Isacoff. 2008. The voltage-gated proton channel Hv1 has two pores, each controlled by one voltage sensor. *Neuron.* 58:546–556. doi:10.1016/j.neuron.2008.03.026

Willumsen, N.J., and R.C. Boucher. 1989. Shunt resistance and ion permeabilities in normal and cystic fibrosis airway epithelia. *Am. J. Physiol.* 256:C1054–C1063.

Willumsen, N.J., and R.C. Boucher. 1992. Intracellular pH and its relationship to regulation of ion transport in normal and cystic fibrosis human nasal epithelia. *J. Physiol.* 455:247–269.

Willumsen, N.J., C.W. Davis, and R.C. Boucher. 1989. Cellular Cl^- transport in cultured cystic fibrosis airway epithelium. *Am. J. Physiol.* 256:C1045–C1053.